WORLD METEOROLOGICAL ORGANIZATION

CIMO/SPICE-IOC-4/INF. 5
(14.VI.2013)

COMMISSION FOR INSTRUMENTS AND METHODS OF OBSERVATION

ITEM: 4

INTERNATIONAL ORGANIZING COMMITTEE (IOC) FOR THE WMO SOLID PRECIPITATION INTERCOMPARISON EXPERIMENT (SPICE)
Fourth Session

Original: ENGLISH

Davos, Switzerland
17 – 21 June 2013

WIND INDUCED ERROR OF PRECIPITATION GAUGES

(Submitted by Vladislav Nespor)

Summary and purpose of document

This document provides information on simulations of wind induced errors on two types of precipitation gauges.

ACTION PROPOSED

The Meeting is invited to invited to note this information and its relevance to the planning of SPICE.

Operational Use of Radar for Precipitation Measurements in Switzerland

Jürg Joss[1]
Bruno Schädler[2]
Gianmario Galli[1]
Remo Cavalli[1]
Marco Boscacci[1]
Edi Held[1]
Guido Della Bruna[1]
Giovanni Kappenberger[1]
Vladislav Nespor[3]
Roman Spiess[3]

Locarno, 23.Sep.1997

[1] MeteoSvizzera, via ai Monti della Trinità 146, CH 6605 Locarno 5 Monti
[2] Landeshydrologie und -geologie, Papiermühlestrasse 172, CH 3003 Bern
[3] Geographisches Institut der ETHZ, Winterthurerstrasse 190, CH 8057 Zürich

10. Wind induced error of precipitation gauges (Nespor)

10.1. Introduction

Gauges are often used as ground-truth reference for radar precipitation estimates. But how true are they? In this chapter investigations of the wind-induced error of measurements for rain and snow, which were made with Hellmann and ASTA precipitation gauges, used in Switzerland, are discussed.

Measurements by precipitation gauges are subject to systematic errors, the most important sources of which are:

1. the deviation of precipitation particles due to wind field deformation around the gauge (wind-induced error),
2. losses caused by wetting of the inner walls of the gauge,
3. evaporation of water accumulated in the gauge container, and
4. splashing of rain drops or blowing of snow flakes out or into the gauge.

The most important component of the systematic errors is the first mentioned error due to wind field deformations (see e.g. Sevruk, 1989), described hereafter.

The strong effect of turbulence can be explained by the air flow around the gauge. This flow is divided into the internal recirculating flow inside the gauge collector, and the external main flow around the gauge. These two flows are separated by a thin layer above the gauge opening. Due to a blocking effect of the gauge, the external air flow is deviated around the gauge and is accelerated. The strongest production of turbulence above the gauge occurs in the shear layer along the separation between the internal and external flows. In the present computation the major effect of the turbulence on the particle motion is to increase its drag (see e.g. Hinze, 1975). Therefore, particles tend to follow the flow more closely in the turbulent regions above and inside the gauge.

The effort needed to estimate wind-induced error of solid precipitation particles is larger than for water drops, because ice crystals and snow flakes are very variable in size and shape. This variety leads to significantly different drag coefficients and density (terminal velocities of free fall) which, therefore, leads to different partial wind-induced error. In general, the terminal velocities of solid precipitation particles are much smaller than those of water drops, resulting in larger wind-induced errors.

In the present work the influence of turbulence on the particle movement was taken into account (Nespor, 1997). The results for rain- and snowfall (snow flakes) allow the determination of the 'true' precipitation intensity (eq.(9.1)) from the known measured intensity, wind speed and type of particle size distribution. The computational results agree well wind-induced errors estimated from field measurements.

10.2. Assumptions

10.2.1.Concept

All computations discussed in this chapter are based on Nespor (1996). In this approach the computation of wind-induced error is divided into the following three steps:

1 - computation of the turbulent flow field around the precipitation gauge using a commercial software package for fluid dynamics (PHOENICS model),

2 - simulation of precipitation particle movement in the computed flow field (determination of the *partial wind-induced error* as a function of the free-stream wind velocity and particle diameter),

3 - integration of partial wind-induced errors over particle size distribution (determination of the *integral wind-induced error* as a function of the free-stream wind velocity, precipitation intensity and parameters of the particle size distribution).

The computations and the subsequent error estimations are based on the following assumptions:

4 - the motion of particles does not affect the air flow, therefore the air flow and the particle motion can be computed separately,

5 - the moving particles do not influence each other, therefore their trajectories can be simulated individually.

Flow fields and particle trajectories were calculated for the properties of air, summarized in TABLE 9.1, and the density of water rw = 999.84 kg m-3. The free-stream turbulence was characterized by the turbulent kinematic viscosity, assumed to be equal to the kinematic viscosity of the air. To simulate the influence of a distorted wind field and of turbulence on the trajectories of falling particles the k-e turbulence model was used (see Nespor, 1996).

TABLE 9.1 : Properties of the air used in the present computations

Temperature	Pressure	Relative humidity	Density	Dynamic viscosity	Kinematic viscosity
[-C]	[kPa]	[%]	[kg m^{-3}]	[kg m^{-1} s^{-1}]	[m^2s^{-1}]
0	101.325	50	1.292	1.718x10-5	1.329x10-5

10.2.2.Properties of snow crystals and snow flakes

In the case of liquid particles (water drops) the distribution of shape, size and terminal velocities are well known. In the case of solid precipitation, the situation is more complicated. In general, the properties of snow crystals depend on meteorological conditions (e.g. humidity, temperature). There is a large variety of natural snow crystals and their classification can be found in Magono and Lee (1966). One of the most compete

descriptions of snow crystal shape properties, relevant to their trajectories, is given by Heymsfield and Kajikawa (1987).

Muramoto et al. (1996) made an interesting study on the size and fall velocity of snow flakes by image processing technique. Their results are based on measurements of a snowfall event lasting 7.5 hours. Although they reported neither the type of snow flakes, nor the detailed structure of snowfall, they measured the density and size distribution of snow flakes. The last two parameters together with the fall velocity are essential for the determination of the precipitation intensity. Their results are in a good agreement with the results of Barthazy et al. (1996), whose measurements were made in real precipitation with a well developed stratiform structure. In addition, the measured data of Muramoto et al. (1996) agree well with the typical range of terminal velocities and densities of snow particles (e.g. Locatelli and Hobbs, 1974; Hobbs, 1974; Goodison and Metcalfe, 1981; Sevruk, 1985). Therefore, the terminal velocities and particle size distribution of Muramoto et al. (1996) seem to be quite representative for an average snowfall.

The summary of measured properties of selected planar crystals, graupel and snow flakes are presented in TABLE 9.2. These data together with empirical relations between the particle mass, particle terminal velocity and particle diameter were used to evaluate partial wind-induced errors in Nespor, 1997.

TABLE 9.2 : Summary of measured particle data
according to Heymsfield and Kajikawa (1987) (ice crystals) and Muramoto et al. (1996) (snow flakes). In the table the particle description code is according to Magono and Lee (1966), T is the air temperature, D is the particle diameter, m is the particle mass, wT is the particle terminal velocity, and rp is the particle density.

Description	T	D	m	wT	ρp
	[-C]	x10-3[m]	x10-6[kg]	[m s^{-1}]	[kg m^{-3}]
Dendrite	---	0.6 - 5.3	0.0007 - 0.108	0.13 - 0.43	20 - 100
rimmed stellar	---	0.7 - 5.3	0.0020 - 0.539	0.19 - 0.72	50 - 150
densely rimmed stellar	---	1.1 - 4.7	0.0310 - 0.905	0.43 - 1.43	100 - 130
lump graupel	>=0.5	0.5 - 4.7	0.0390 - 17.200	0.70 - 4.40	210 - 630
	< 0.5	0.5 - 9.0	0.0140 - 68.000	0.47 - 4.65	89 - 350
conical graupel	>=0.5	1.1 - 7.5	0.1650 - 110.000	1.07 - 5.70	210 - 630
	< 0.5	0.8 - 8.6	0.0580 - 53.700	0.64 - 4.08	89 - 350
snow flakes	---	0.5 - 15.0	0.0019 - 12.740	0.43 - 1.51	48 - 190

10.2.3.Particle size distribution

The particle size distribution is very important to determine snowfall intensity and estimate the integral wind-induced error. Because of the large variety of solid precipitation particle types occurring in real precipitation events, and because of difficulties with measurements, the information about solid particle size distributions in literature is rare. Our calculations are based on the particle size distribution of snow flakes presented in Muramoto et al. (1996), whose measurements were made during a snowfall event lasting 7.5 hours. Their size distribution was fitted by the gamma

distribution, and the result was used to find wind-induced errors for the Hellmann and ASTA gauges in the present study.

10.3. Results

10.3.1. Liquid precipitation particles

For Hellmann and ASTA precipitation gauges flow fields were computed for the free-stream velocities ranging between vf = 0.5 and 12 m s-1. In the case of rain drops minor modifications were made in the source code for particle trajectory computation (model PHOENICS, see "9.2 Assumptions") in order to include the influence of turbulence on the particle motion. Computations of partial wind-induced errors and the subsequent integration over the drop size distribution resulted in the integral wind-induced error as a function of rainfall intensity R, the free-stream wind speed and the parameter k in the Ulbrich drop size distribution (Ulbrich, 1983, eq.(9.2)). The results showed that the error increases with increasing wind speed. Moreover, smaller rain rates and cases with lower parameters k have a larger contribution from small drops to the precipitation amount and, therefore, larger wind-induced errors (see Nespor, 1996, 1997).

For practical use it is convenient to express the rainfall rate as

$R = n \cdot R_m$ (9.1)

where R_m is the rate of rainfall measured by the gauge, n is the multiplication factor and R is the ÕtrueØ rain rate, intended as the desired precipitation flux across a large area, i.e. without boundary effects caused by the instrument. The integral wind-induced errors are presented in Figure 9.1. It can be used to correct the measured rain rates (amounts) if κ and ν_f are known.

Comparing the multiplication factors of the two gauge types (Figure 9.1) shows slightly larger values for the ASTA gauge, indicating a lower efficiency of the ASTA compared to the Hellmann gauge. This is probably caused by the different constructions: although the Hellmann and ASTA gauges have the same orifice area, the body of the ASTA gauge has a larger outer diameter because of the heating and, therefore, introduces the larger disturbance to the air flow.

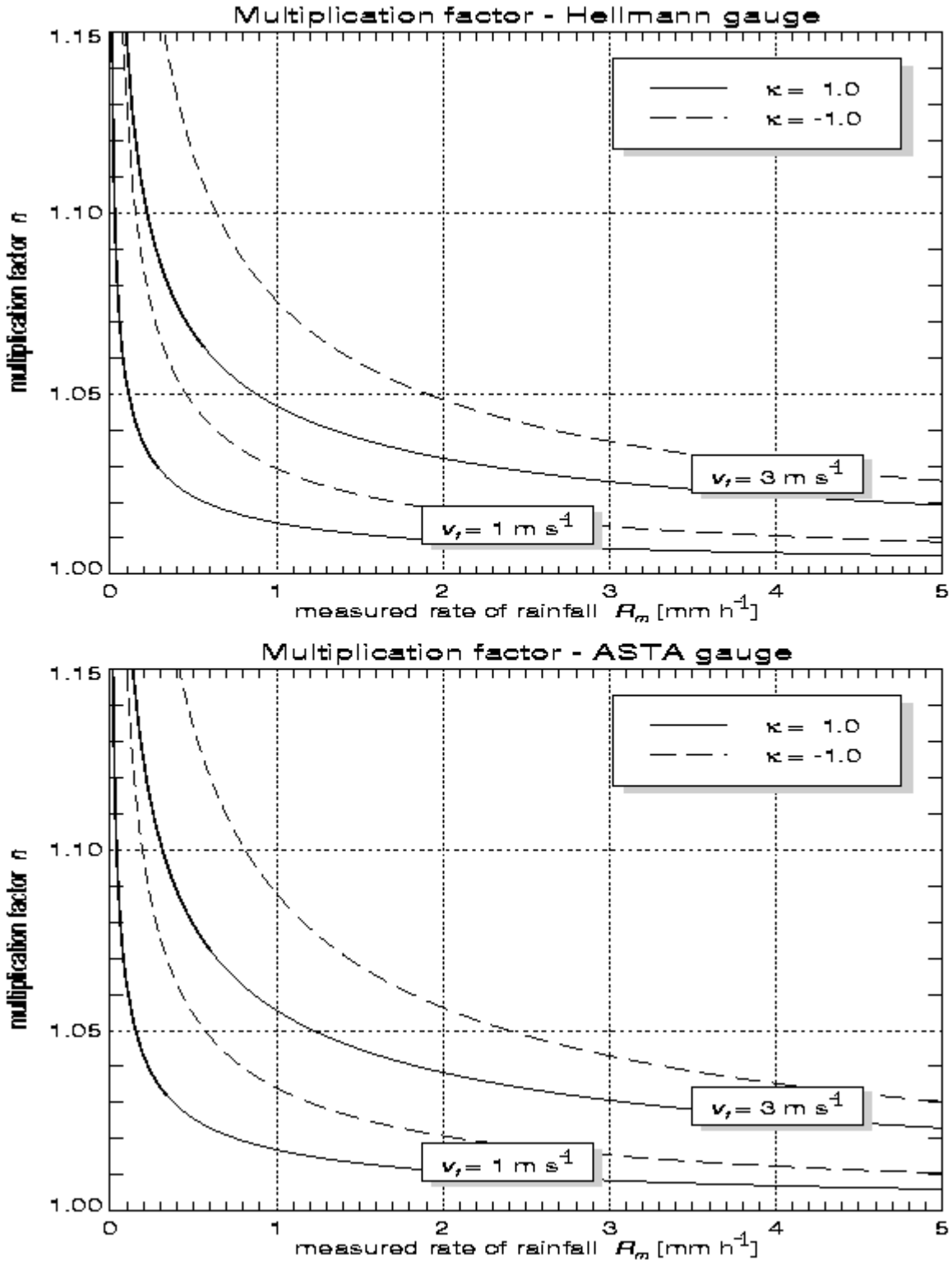

: The multiplication factor n in eq.(9.1) of the Hellmann (top) and ASTA (bottom) precipitation gauges is plotted as a function of the measured rate Rm. The multiplication factors were derived from the computed integral wind-induced errors. The drop size parameter k = -1 in eq.(9.2) is

typical for orographic rain (with a larger fraction of smaller drops), and k = 1 for a thunderstorm rain (with a larger fraction of larger drops, parametrization described by Ulbrich, 1983).

10.3.2.Results for solid precipitation particles

In contrast to water drops, ice crystals and snow flakes have a larger variety of forms and densities. Therefore, large modifications in the calculation of trajectories (see "9.2.1 Concept") were necessary. In the first step the partial wind-induced errors were evaluated. Again, the computations were concentrated on the Hellmann and ASTA precipitation gauges, and on those solid particles for which information about the particle shape, density (or mass), and terminal velocity was completely available (Heymsfield and Kajikawa, 1987; Muramoto et al., 1996).

The results for various ice crystals produced larger multiplication factors than rain drops. Generally, for lower terminal velocities, the partial wind-induced error is also larger. Lighter dendrites cause higher errors: less than 20% of the particles were caught by gauges for vf = 1.0 m s-1, while the heavier lump graupels produced much smaller errors (Nespor, 1997).

A snowfall event can contain a variety of different types of ice crystals and snow flakes, determined to a great extent by the prevailing conditions at the location of particle generation, and by the layers of the atmosphere through which the particles pass on their way to the ground. This extreme variability introduces large insecurities, both to measurements of snowfall and to modelling studies, as has already been mentioned above ("9.2.2 Properties of snow crystals and snow flakes"). The results presented here for snow are therefore less reliable than those in the previous section for rain.

The partial wind induced error for different diameters of snow flakes (Muramoto et al., 1996) was evaluated for wind velocities vf = 0.5, 1.0, 1.5, 2.0 and 3.0 m s-1. The computed values of partial wind-induced error were fitted to a gamma probability density function (see Nespor, 1996).

In the Ulbrich drop size distribution (eq.(9.2)) parameter k determines the type of rain. The only parameter that depends on the rate of rainfall is L (Ulbrich, 1983).

$$N_{(D)} = N_0 \cdot D^{\kappa} \cdot \exp(\Lambda D) \qquad (9.2)$$

In the present computations we assumed that this type of distribution found in rain is valid also for the size distribution of snow flakes and that the values of L varied between 350 and 1400[m-1]. This corresponds to R between approximately 8.6 and 0.03 mm h-1.

Similarly to water drops the integral wind-induced error for snow flakes increases with increasing wind velocity and decreasing snowfall intensity, but for R between 1 and 5 mm h-1 the increase of the error is lower compared to water drops. In general, the errors for snow flakes are 5 to 10 times larger than the errors for water drops (Nespor, 1997). Figure 9.2 shows the multiplication factor n as a function of the measured rate of snowfall R_m and wind velocity vf. The ÕtrueØ rate of snowfall R is then obtained from the eq.(9.1). Similarly to rain the ASTA gauge have a larger wind-induced error (larger n values) than the Hellmann gauge.

10.4. Comparison with measurements

10.4.1. Rainfall

The comparison of computational results and field measurements of wind-induced error of rainfall in Figure 9.3 is based on the study of Sevruk (1989). In this study the wind-induced error is estimated from paired measurements: comparison of the results of a Hellmann gauge elevated to 1.5 m above the ground with those of a Hellmann gauge at ground level. The estimates were based on the 10-year data recorded in Les Avants (Switzerland). Precipitation data were divided into classes according to rain rate and wind speed at the gauge orifice (see Sevruk, 1989). The error is expressed as the difference between the gauge amounts at ground level minus the elevated one divided by the ground level amount. Figure 9.3 shows computed and measured wind-induced errors for average wind speeds of 2.5 and 3.5 m s-1. The curves in each figure indicate the expected boundaries for the measurements. They were computed for the parameter k = -1 and a free-stream velocity (vf) which is 0.5 m s-1 larger than the corresponding wind speed class average, and for the parameter k = 1 and a free-stream velocity 0.5 m s-1 smaller than the corresponding wind speed class average. Although the measured data are based on averages and a closer information about the type of precipitation (drop size distributions) was not available, they agree quite well with values derived from computations.

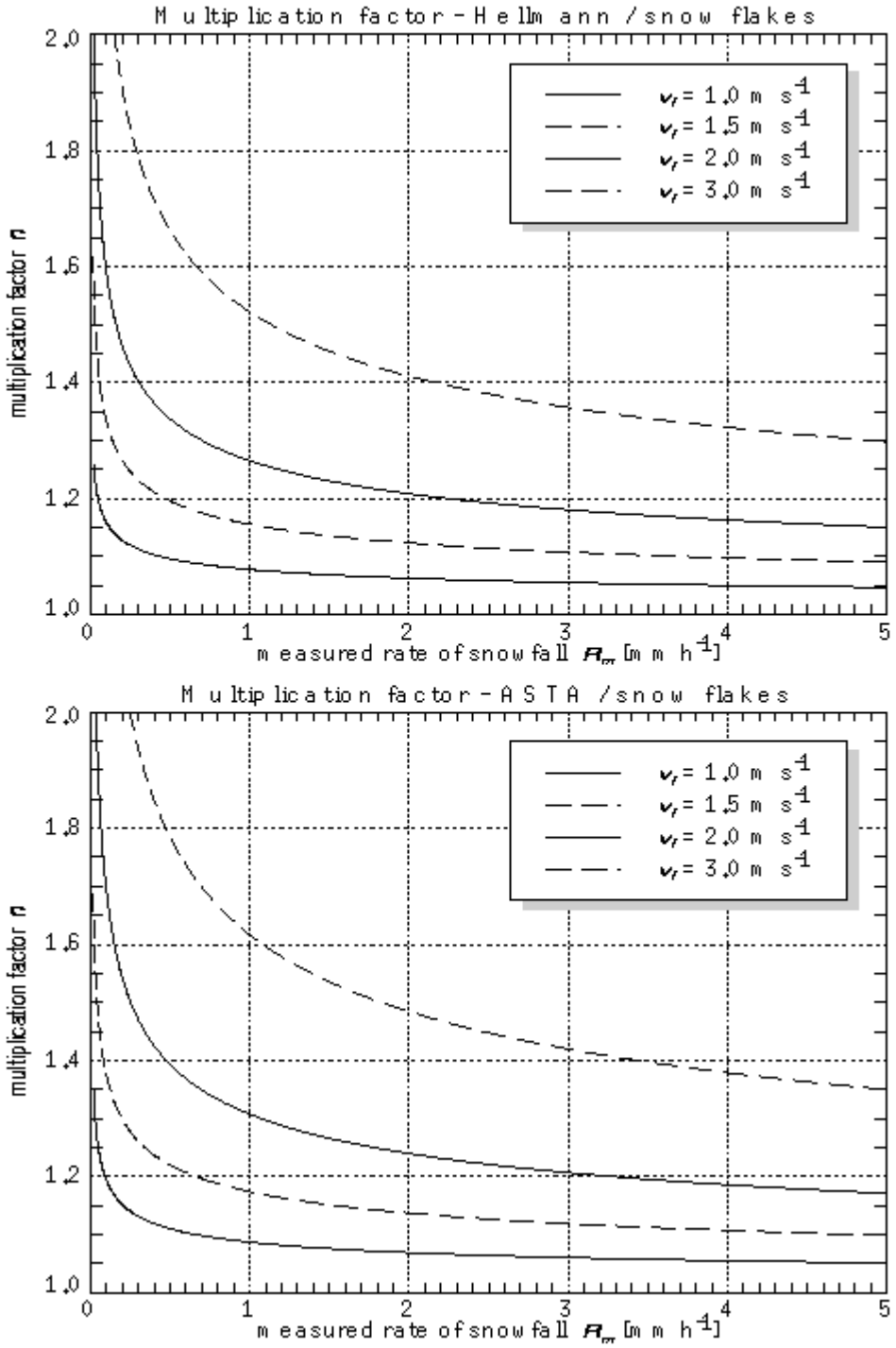

Figure 9.2: The multiplication factor n in eq.(9.1) of the Hellmann (top) and ASTA (bottom) precipitation gauges is plotted as a function of the measured rate of snowfall Rm the multiplication factors were derived from the computed integral wind-induced errors.

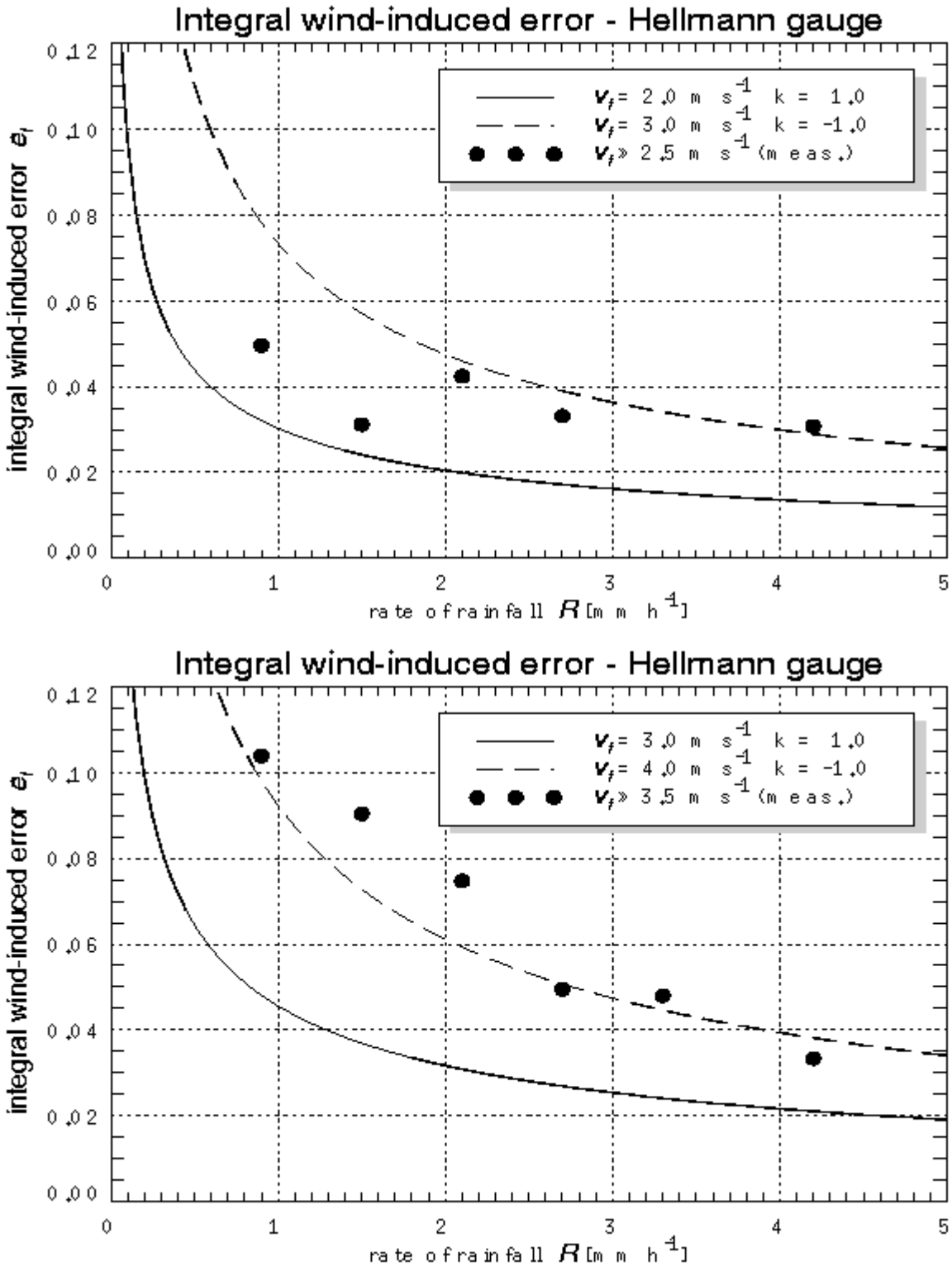

Figure 9.3: Computed integral wind-induced error of rainfall and values estimated from measurements (Sevruk, 1989). The measured values (points) are class averages of several rainfall events for the free-stream velocity of vf = 2.5 m s-1 (top) and vf = 3.5 m s-1 (bottom). The curves represent approximate boundaries for the parameter k = -1 and the free-stream

velocity 0.5 m s-1 larger than the measured class average (dashed line), and for the parameter k = 1 and the free-stream velocity 0.5 m s-1 smaller than the measured class average (solid line)

10.4.2.Snowfall

In the case of snowfall the present comparison of computed errors and field measurements is based on the study of Guenther (1993), a part of the WMO solid precipitation intercomparison project (e.g. WMO/CIMO, 1996). The wind-induced error was obtained from the difference between the Hellmann precipitation gauge elevated 1.0 m above the ground, and the reference measurement by the Double Fence Intercomparison Reference (DFIR) (see e.g. Yang et al., 1994). The original snowfall data measured in the period 1986-1993 in Herzgerode (Germany) were subdivided according to air temperature and fitted by lines. The solid line in Figure 9.4 represents the resulting fit for the air temperature of 0- C. The points are computed integral errors for the snowfall intensity of 0.5 and 1.0 mm h-1, respectively. Although snowfall intensities of measurements were not published, it can be expected that they were mostly between 0.5 and 1.0 mm h-1. For example, Maurer (1993) reported the mean snowfall intensity of approximately 0.8 mm h-1 for 56 precipitation events in the period of two years. Therefore, the intercomparison in Figure 9.4 shows good agreement between computations and field measurements.

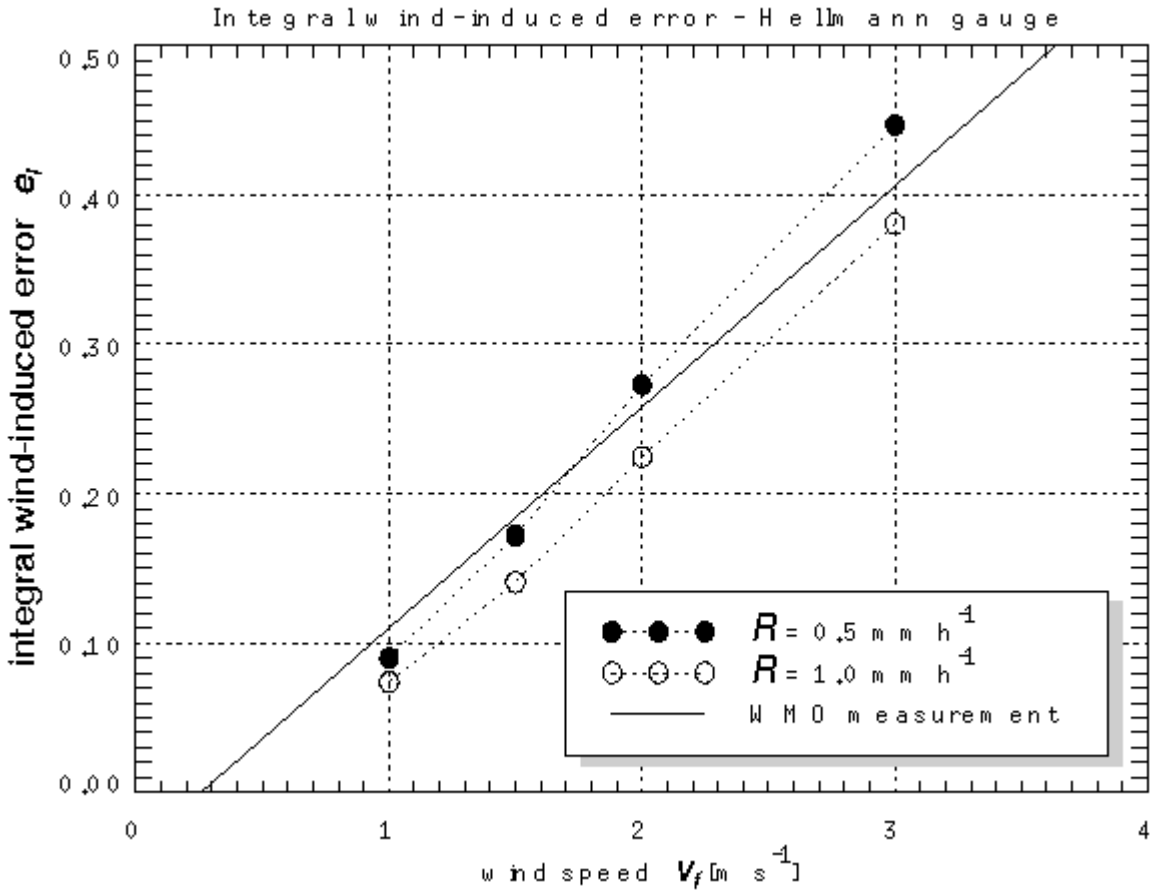

Figure 9.4: Comparison of the computed wind-induced error of snowfall and results based on

measurements (WMO, Guenther, 1993). The solid line approximates the measured data for the air temperature of 0- C, the points represent computed values of integral wind-induced error for the snowfall intensity of 0.5 mm h-1 (filled points) and 1.0 mm h-1 (empty points).

10.5. Conclusions

The present study uses a further numerical simulation to find the wind-induced error of precipitation measurements. The comparison of computed results with error estimates based on field measurements shows good agreement. The computational results can be used to correct measured precipitation amounts if the input parameters are known. The results are presented in the form of a multiplication factor as a function of the measured rate of precipitation and wind speed (Figure 9.1 and Figure 9.2). The computations of the wind-induced errors in snow were based on one well documented precipitation event. As discussed in Sec.9.3.2 "Results for solid precipitation particles" on page 96, the measured parameters (the range of densities and terminal velocities of the snow flakes, and the particle size distribution) are quite representative for an average snowfall. Therefore, the diagrams can be used more generally.

The numerical simulation confirmed that there are differences between precipitation gauges. In general, the ASTA precipitation gauge shows slightly higher wind-induced errors than the Hellmann gauge (higher multiplication factors n in eq.(9.1)). This is caused by the larger flow disturbance introduced by the ASTA gauge body containing the heating elements. Furthermore, the computations confirmed that the wind-induced errors depend strongly on the free-stream velocity at the level of the gauge orifice, and on the weight and shape of precipitation particles. For the same free-stream velocity the lighter snow flakes show an integral wind-induced error 5 to 10 times larger than water drops. There are also differences between various snow crystals, the lighter crystals exhibit a higher wind-induced error.

Limitations of the presented procedure are caused by the fact that the input parameters such as the wind speed at the gauge orifice, the precipitation rate and particle sizes are not known. There would be a possibility to eliminate this uncertainty partially by replacing the input parameters by some representative averages. But to do that, further investigations on real precipitation events are needed. Little is known yet about the size distribution of particles and its variation with time, especially in the case of snowfall.

The presented procedure to estimate errors can also be used to check the performance of existing precipitation gauges, to improve the shape of precipitation gauges, to investigate the influence of different wind shields, and to develope and verify new correction procedures. Last but not least, the results are essential for the interpretation of radar-gauge comparisons.